CRYSTAL GROWTH & DESIGN
2007
VOL. 7, NO. 9
1590−1598

Polymorphism and Crystallization of Famotidine

Jie Lu,* Xiu-Juan Wang, Xia Yang, and Chi-Bun Ching

School of Chemical and Biomedical Engineering, Nanyang Technological University, Singapore 637459

Received November 30, 2006; Revised Manuscript Received February 5, 2007

ABSTRACT: Famotidine crystallizes in two different polymorphic forms: the metastable polymorph B and the stable polymorph A. In this work, solid characterization for both polymorphs has been conducted in detail. The solubility, metastable zone width and interfacial energy of both polymorphs in different solvents have been measured. The influence of solvent, cooling rate, initial concentration, nucleation temperature, and seeding on polymorphism has been investigated. Experimental results show that the nature of polymorph that crystallizes from solution depends on the initial concentration, solvent, cooling rate, nucleation temperature, and seeding strategy. In addition, the polymorphic transformation from polymorph B to polymorph A in slurry is slow, and yet can be accelerated by increasing temperature and seeding with polymorph A.

Introduction

Polymorphism may be defined as the ability of a compound to exist in different crystalline forms in which the molecules have different arrangements (packing polymorphism) and/or conformations (conformational polymorphism) in the crystal lattice.[1] Polymorphism is a widespread phenomena observed for more than half of all drug substances.[2] Polymorphs can have different mechanical, thermal, physical, and chemical properties, such as compressibility, melting point, crystal habit, color, density, dissolution rate, and solubility. These can have a great influence on the bioavailability, hygroscopicity, stability, filtration, and tableting processes of pharmaceutical materials.[3]

In experimental and industrial practice, it is commonly observed that the metastable form appears instead of the stable form, and this has been stated as a rule known as the Ostwald rule of stages.[4] According to Ostwald's Rule, in a crystallization from the melt or from solution, the solid first formed will be that which is the least stable of the polymorphs, the one with the largest Gibbs free energy. Although it is a useful indicator of a possible sequence of production of crystalline forms, it is not as universal and reliable.[5]

The traditional methods, such as varying solvent,[6] temperature,[7] supersaturation,[8] cooling rate,[9] and seeding strategy,[10,11] have been extensively applied to control the polymorphic behavior of a pharmaceutical material during its crystallization process.[12] Recent approaches for discovery and selection of polymorphic forms of a compound include crystallization with tailor-made soluble additives,[13−16] polymer heteronuclei,[17,18] crystallization on various substrates and templates,[19−21] laser-induced nucleation,[22] solvent drop grinding,[23] spray drying,[24] supercritical fluid crystallization,[25] capillary crystallization,[26,27] crystallization confined in nanopores,[28] etc. In spite of the above great efforts, the fundamental mechanisms and molecular properties that drive crystal form diversity, specifically the nucleation of polymorphic forms, are not well-understood. As a result, the appearance and disappearance of polymorphs are still experienced as somewhat mysterious and predictive methods of assessing polymorphic behavior of pharmaceutical compounds remain a formidable challenge.[29,30]

Famotidine, which is an excellent histamine H_2 receptor antagonist,[31] has been chosen as the model substance because only a very limited proportion of the literature on antihistamine agents has been devoted to the problematic issue of polymorphism.[32] Famotidine has two known conformational polymorphs (A and B), but the system is far from well-established and understood. According to Overgaard and Hibbs,[32] crystals of polymorph A and polymorph B belong to the monoclinic crystal system. The unit-cell dimensions of polymorph A are a = 11.912 Å, b = 7.188 Å, c = 16.624 Å, β = 100.045°, whereas the unit-cell dimensions of polymorph B are a = 16.980 Å, b = 5.285 Å, c = 17.639 Å, β = 116.416°. The crystal packings and conformers of polymorph A and polymorph B are shown in Figure 1.

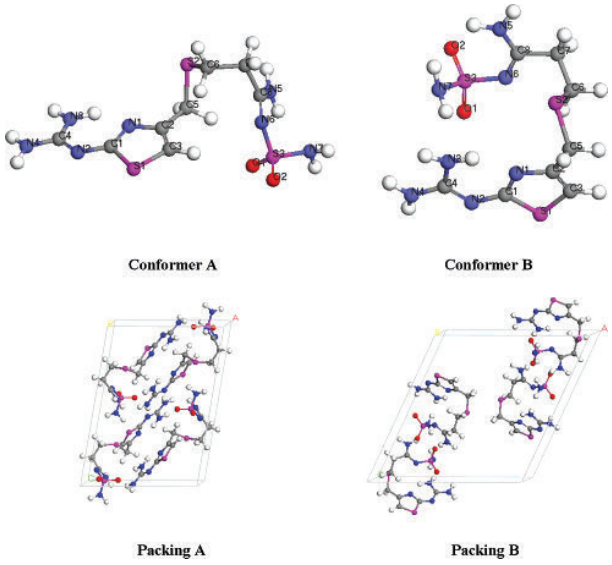

Figure 1. Crystal packings and conformers of famotidine polymorphs.

The aim of this work is to study the influence of the crystallization process parameters on the polymorphism of famotidine. The operating parameters studied are the solvent, cooling rate, initial concentration, nucleation temperature, and seeding. Finally, the "polymorphic window" for the crystallization of famotidine from aqueous solution is described and discussed.

Experimental Section

Materials. Form B of famotidine, methanol, and acetonitrile were obtained from Sigma-Aldrich (St. Louis, MO). All chemicals were of the highest grade available and used without further purification. Form

* To whom correspondence should be addressed. Fax: +65 6794 7553. E-mail: lujie@ntu.edu.sg.

10.1021/cg060865+ CCC: $37.00
Published on Web 05/15/2007

A was slowly recrystallized from dilute acetonitrile solution. Deionized water was prepared with a Milli-Q water system (Millipore, Billerica, MA).

Powder X-ray Diffraction. PXRD was conducted by a Bruker D8 Advance diffractometer (Bruker, Germany) at 40 kV and 30 mA with a Ni-filtered Cu Kα radiation source ($\lambda = 1.54$ Å). The samples were scanned from 5 to 40° 2θ at a step size of 0.05° and at a scanning rate of 3°/min.

Fourier-Transform Infrared Spectroscopy. FTIR spectra were recorded from KBr disks using a Digilab Excalibur Series FTS-3000 spectrophotometer (Digilab, Canton, MA). Ground KBr powder was used as the background in the measurements. The number of scans was 32 and the resolution was 4 cm^{-1}. The measured wave number range was from 4000 to 400 cm^{-1}.

To construct the calibration curve for quantitative analysis, we selected the characteristic peaks at 926 and 943 cm^{-1} for pure A and B forms, respectively. The reference peak at 906 cm^{-1}, common to both forms, was selected as an internal standard. And the following equation was used for calibration

$$Y = \frac{a'bc'}{ab'c + a'bc'} \quad (1)$$

where a and a' are the intensities of the reference peak at 906 cm^{-1} of pure A and B forms, respectively, b and b' are the intensities of the peak at 926 cm^{-1} of the pure A form and the sample, respectively, and c and c' are the intensities of the peak at 943 cm^{-1} for pure B form and the sample. Y is the calculation factor. The calibration curve was thus obtained from plotting the calculation factor Y against the concentration of form B in standard samples. The standard samples were prepared as mixtures of the two polymorphs, in various mass fractions: 0.00, 17.5, 31.0, 43.5, 65.7, 84.2, and 100 wt % form B in the mixture. The mixing was done by hand for more than 10 min.

Thermal Analysis. Thermal analysis methods used in this study included differential scanning calorimetry (DSC), thermogravimetric analysis (TGA), and hot-stage microscopy (HSM). DSC was performed using a Mettler-Toledo DSC-822 differential scanning calorimeter (Mettler-Toledo, Columbus, OH). Indium was used for calibration. Accurately weighed samples (5−8 mg) were placed in hermetically sealed aluminum pans and scanned at 10 °C/min under a nitrogen purge. TGA was conducted with a Shimadzu TGA-50 instrument (Shimadzu, Japan) that was also calibrated with indium prior to analysis. The sample weight was approximately 10−20 mg and a heating rate of 10 °C/min under nitrogen purge was used. HSM analysis was carried out with a Linkam THMS 600 hot-stage (Linkam, UK) and an Olympus BX51 microscope with an attached CCD video camera (Olympus, Japan), and images were recorded and analyzed by software (analySIS). The powders of the A and B forms were heated at 3 °C/min to 190 °C, held for 5 min, cooled at 3 °C/min to 70 °C, and reheated at 3 °C/min to 190 °C.

Raman Spectroscopy. Raman spectra were collected using a Renishaw System 1000 micro-Raman spectroscope (Renishaw, U.K.) equipped with an Ar-ion laser (514.5 nm) with an output power of 50 mW. Calibration was performed using a silicon standard. Measurements were made using a 1200 lines/mm grating.

Scanning Electron Microscopy. The morphology of each crystalline form was observed by scanning electron microscopy (SEM). A small amount of samples were scattered on double-sided adhesive carbon tabs mounted on SEM stubs and coated with Au/Pd in a Cressington 208 sputter coater (Pelco International, Redding, CA). Thereafter, the samples were examined with a JSM-6700F Field Emission SEM (Jeol, Japan) operating at 15 kV.

Solubility Measurements. The solubility of the two polymorphs of famotidine was measured in water, methanol, and acetonitrile at various temperatures. A saturated solution of the pure solid form was prepared in a 30 mL jacketed glass crystallizer. The Teflon-coated magnetic stirring bar ensured proper mixing in the crystallizer. The temperature of the crystallizer was controlled by a heating and refrigeration circulator (PolyScience, Niles, IL), and the solution was stirred for at least 24 h at each temperature. After the equilibration, the agitation was stopped, and the solution was allowed to settle for 6 h. The supernatant in equilibrium with a macroscopically observable solid was then filtered through Millex-VV 0.1 μm filters (Millipore, Billerica, MA). The concentration of filtered supernatant was determined spectroscopically by measuring the absorbance at 280 nm of UV spectroscopy (Shimadzu, Japan). The extinction coefficient obtained through calibration experiments was 35.6 mL/(mg cm). Calibration curve was determined in pure water. The solubility of each sample was measured in duplicate.

Metastable Zone Width Measurements. The experiments were carried out in a 50 mL jacketed glass crystallizer. The temperature control of the crystallizer was performed by a programmable circulator (Julabo, Germany). For all experiments, the stirring rate was taken as being equal to 500 rpm. A laser generator (Interlink TS−N, Singapore) generating a laser beam of 660 nm was applied to detect turbidity. The saturated solutions of the pure polymorph B prepared at various temperatures were heated 3 °C above the solubility temperatures. The solutions were then cooled at a constant rate of 12 °C/h. When the solutions became translucent, the temperatures were recorded, and the crystals were filtered off immediately and analyzed by FTIR.

Induction Time Measurements. The time at which the crystals were detected in the solution was noted as the induction time, t_{ind}. A suspension of the desired amount of the polymorph B of famotidine was heated 3 °C above the equilibrium temperature to dissolve all crystals. It was then filtered through a 0.1 μm membrane filter and added to the 30 mL jacketed glass crystallizer, the temperature of which was kept at the desired value. When crystals appeared, the time was recorded, and the crystals were filtered off immediately and analyzed quantitatively by FTIR for their polymorphic content. Experiments under each set of conditions, defined by supersaturation ratio S and nucleation temperature T, were duplicated. The supersaturation ratio was calculated as $S = c/c_{eq}$, where c and c_{eq} are the initial concentration of famotidine and the equilibrium solubility at nucleation temperature T of the solid phase appearing in the experiment, respectively. The reported induction time, t_{ind}, is the average of duplicate measurements.

Cooling Crystallization Experiments. The experiments were performed in the 50 mL jacketed glass crystallizer described above. The cooling rates employed were 2, 12, 20, and 60 °C/h, and quench-cooling by use of an ice bath. As for the cooling crystallization without seeding, the crystals that first appeared were filtered off and analyzed quantitatively by FTIR for their polymorphic content. Furthermore, in some experiments, the crystals were allowed to remain suspended for continuing cooling before being collected for analysis. The other variable crystallization parameters investigated were the initial concentration and solvent.

As to the seeding experiments, the initial saturate temperatures of B-form in water were set at 50, 70, 90, and 94 °C, respectively. The cooling rates employed were 2 and 20 °C/h, respectively. The used seeds were not ground to increase the surface area because of the transformation that may occur. The amount of seeds corresponding to the solubility of the B form ranged from 1 to 30%. The point of addition of the seeds was roughly estimated from solubility data and the width of the metastable zone.

Solvent-Mediated Polymorphic Transformation. First, the suspensions of the excess amount of pure polymorph A or B in water, methanol, or acetonitrile were shaken by a wrist-action shaker (Burrell, Pittsburgh, PA) at approximately 200 strokes per minute. A portion of each suspension was withdrawn and filtered at designated times, and the polymorphic composition of the solid phase was determined by FTIR. At temperatures of 40 and 60 °C and after 14 days, no interconversion was observed in the suspension of pure polymorph.

Second, the suspensions of polymorphic mixtures were employed. Saturated aqueous solutions of the B form were prepared in the 50 mL jacketed glass crystallizer at 40 and 60 °C, respectively. The mixtures of both forms in known ratios were then added into the saturated solutions. The suspension density of the slurries was about 6 mg/mL. The agitation rate was 500 rpm. The temperature was controlled by a Julabo circulato, and kept constant. A small amount of slurry was periodically withdrawn, filtered, dried, and quantitatively analyzed by FTIR.

Results

Solid Characterization of Pure Polymorphs. Figure 2 shows typical PXRD patterns for the two polymorphs of famotidine. For example, the A and B forms have characteristic diffraction peaks at 10.66 and 5.94°, respectively.

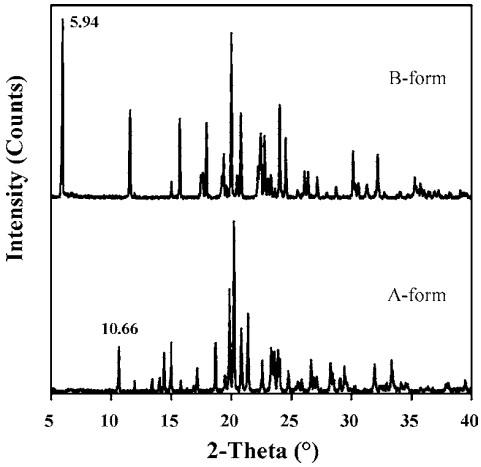

Figure 2. Powder X-ray diffraction patterns for A and B forms of famotidine crystals.

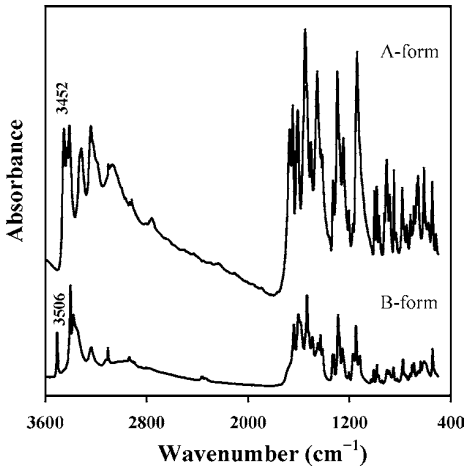

Figure 3. FTIR spectra of A and B forms of famotidine crystals.

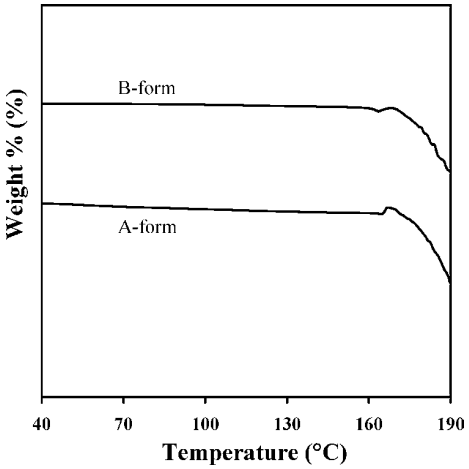

Figure 4. TGA curves of A and B forms.

The IR spectra of two polymorphs are shown in Figure 3. For instance, the A and B forms have characteristic absorption bands at 3452 and 3506 cm^{-1}, respectively.

Typical TGA and DSC thermograms of the two polymorphs of famotidine are shown in Figures 4 and 5, respectively. The measured onset and peak maximum of the melting endotherm

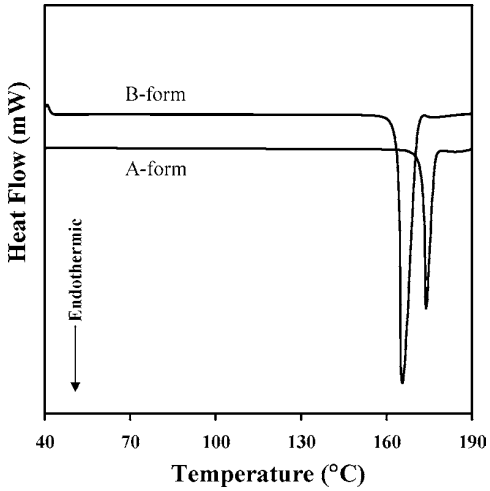

Figure 5. DSC curves of A and B forms.

of polymorph A are 166.9 and 173.8 °C, respectively, whereas those of polymorph B are 158.9 and 165.4 °C, respectively. The measured melt enthalpy of polymorphs A and B are 49.7 and 48.6 kJ/mol, respectively. Results from the hot-stage microscopy experiments confirm that the B form has a lower melting point, as shown in Figure 6.

Raman spectra of pure A and B form in the range of 300−1600 cm^{-1} are presented in Figure 7. Some specific differences between the A and B forms can clearly be observed. For instance, the peaks at 327, 362, 545, 659, 750, 1258, and 1465 cm^{-1} are characteristic of the A form and the peaks at 353, 549, 684, 740, 1241, and 1455 cm^{-1} are characteristic of the B-form. The region from 300 to 400 cm^{-1} is sensitive to crystal structure and contains peaks due to lattice vibrations. The bulk of the chemical structure details can be obtained from the region 500 to about 1600 cm^{-1}. The large differences in Raman spectra of the two forms of famotidine are mainly caused by the conformational differences of the molecules in the crystal lattice of the A and B form. The molecular conformations are significantly different through a torsion angle at C6−C7 in the main carbon chain.

The morphology of each form is shown in Figure 8. Both forms mainly exhibit a rodlike morphology, and thus it is difficult to identify the polymorph by the shape of the crystal. Furthermore, the A form has smaller size and is apt to aggregate.

Calibration Curve for Quantitative Analysis. The calibration curve plotted in Figure 9 exhibits good linearity over nearly the entire concentration range studied, which suggests that the simple approach applied in this work for the quantification of the polymorphic mixture of famotidine via FTIR is practical.

Solubility of Polymorphs. Figure 10 presents experimental results over the solubility of the two forms of famotidine in water, methanol, and acetonitrile at different temperatures. The solubility curves expose a monotropic nature of the polymorphs of famotidine. Polymorph A is the thermodynamically favored form (stable form), whereas polymorph B is the kinetically favored form of famotidine (metastable form).[33]

The solubility of both polymorphs increase with temperature. Using the van't Hoff relation $\ln x = -(\Delta H^{diss}/RT) + (\Delta S^{diss}/R)$ for the solubility curves of Figure 10, we obtained the dissolution enthalpies and dissolution entropies of both polymorphs, as list in Table 1. The differences in dissolution enthalpy and dissolution entropy of both polymorphs are negligible.

Metastable Zone Width. Figures 11−13 show the metastable zone widths of the polymorphs of famotidine in three solvents

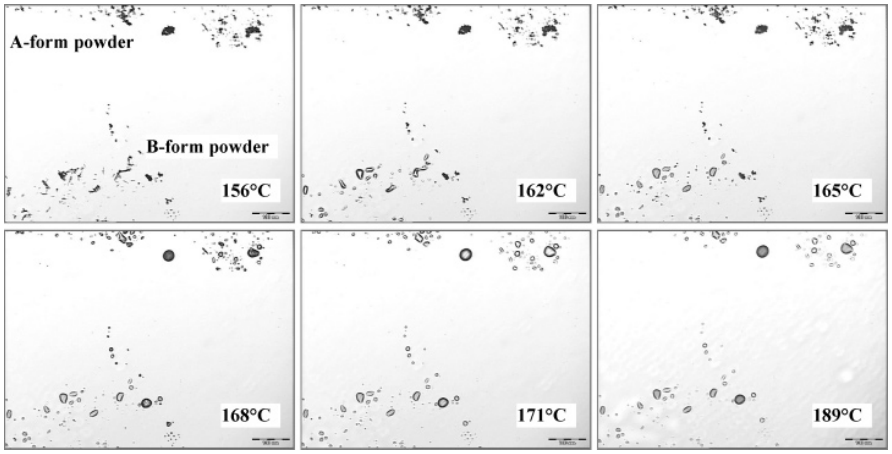

Figure 6. Melting behaviors of A and B forms examined under HSM.

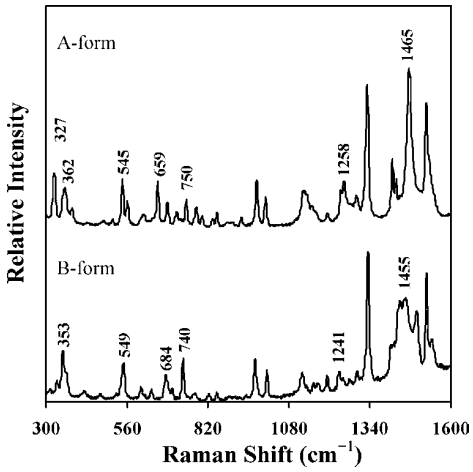

Figure 7. Raman spectra of famotidine polymorphs.

at a cooling rate of 12 °C/h. The average metastable zone widths of polymorph A in methanol, water, and acetonitrile are 20.5, 15.6, and 44.5 °C, respectively. On the other hand, the average metastable zone width of polymorph B in water is about 3.0 °C, which is much narrower than that of polymorph A. The higher the nucleation barrier, the larger the metastable zone width of the polymorph is.[34] Therefore, the nucleation barrier of polymorph A of famotidine is larger than that of polymorph B.

Induction Time. Usually, the induction time t_{ind} is interpreted as the time for critical nucleus formation plus the time for growth to a detectable size.[35] When the formation of a stable nucleus is the rate-limiting step, the induction time is inversely related to the nucleation rate J.[36] Therefore, according to the classical nucleation theory, t_{ind} is related to the supersaturation ratio, S, the temperature, T, and the interfacial tension, γ, between the nucleus and the supersaturated solution according to eq 2[37]

$$J = \frac{1}{t_{ind}} = A_n \exp\left(-\frac{\gamma^3 \upsilon_m^2}{\nu^2 \kappa_B^3 T^3 (\ln S)^2}\right) \quad (2)$$

where A_n is a pre-exponential coefficient, β is a geometric factor, υ_m is the molecular volume of the solute, ν is the number of ions into which a solute molecule dissociates ($\nu = 1$ for famotidine molecule), and κ_B is the Boltzmann constant.

Assuming the critical nuclei are spherical, a plot of $\ln(t_{ind})$ against $1/(\ln S)^2$ should yield a straight line of slope $(16\pi\gamma^3\upsilon_m^2)/(3\kappa_B^3T^3)$, from which γ can be calculated. The plots of $\ln(t_{ind})$ against $1/(\ln S)^2$ at 0 and 50 °C in three solvents are illustrated in Figure 14, and the calculated γ are list in Table 2.

Figure 14 shows that, at the nucleation temperature of 50 °C, the nature of the polymorph that nucleates depends on S of the initial solution. At low S, polymorph A nucleates, whereas at high S, polymorph B nucleates. As shown in Table 2, at the same nucleation temperature, among the three solvents studied, the interfacial tension between aqueous supersaturated solution and the nucleus of polymorph A is highest. Meanwhile, the interfacial tension is also found to decrease with an increase in temperature. Against expectation, the calculated interfacial tension of polymorph B is higher than that of polymorph A. Through inverse gas chromatographic analysis, Tong et al.[38] have demonstrated that the metastable polymorph of salmeterol xinafoate possesses a higher surface free energy, higher surface entropy, and a more polar surface than the stable polymorph.

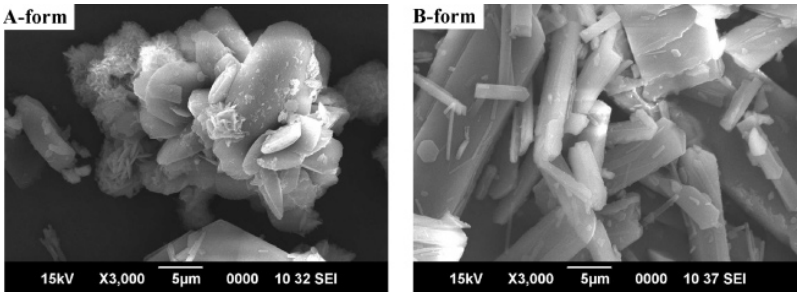

Figure 8. SEM photographs of the two polymorphs of famotidine.

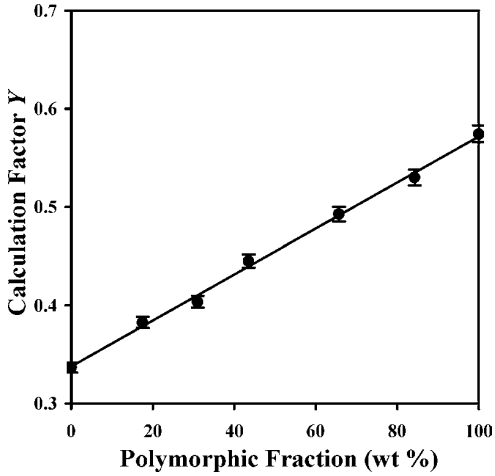

Figure 9. Calibration curve established by plotting the calculation factor Y versus the polymorphic fractions of form B in the samples.

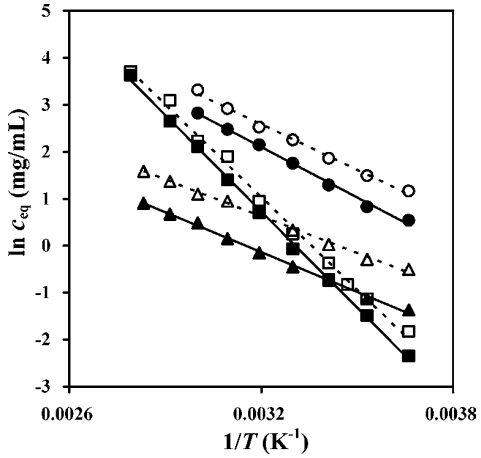

Figure 10. van't Hoff plots of equilibrium solubility of polymorphs A and B against the reciprocal of absolute temperature: (○) B in methanol; (●) A in methanol; (□) B in water; (■) A in water; (Δ) B in acetonitrile; (▲) A in acetonitrile.

Table 1. Dissolution Enthalpies and Entropies of Polymorphs in Different Solvents

	water		methanol		acetonitrile	
dissolution params	A form	B form	A form	B form	A form	B form
dissolution enthalpy, ΔH^{diss} (kJ/mol)	57.5	56.6	29.8	26.9	23.8	20.4
dissolution entropy, ΔS^{diss} (J/mol)	189.6	190.2	112.6	107.5	75.0	70.2

Polymorphic Window. From the experiments of induction time measurement, the "occurrence domain"[39] of each respective polymorph with respect to nucleation temperature and initial concentration, designated as "polymorphic window" in this work, can be determined. To control a crystallization process to produce the desired polymorph, the polymorphic window that is unique for that particular polymorph needs to be delineated. The polymorphic window for the crystallization of famotidine from aqueous solution is described in Figure 15.

As shown in Figure 15, the line AD intersects the supersaturate curve of B-form, the boundary between zones I and II, and the boundary between zones II and III at points B, C, and D respectively, at which the nucleation temperatures are noted as T_B, T_C, and T_D. When a saturated solution at point A is cooled, the polymorph of crystalline product is B form when the nucleation temperature is between T_B and T_C, a mixture of A and B forms when the nucleation temperature between T_C and T_D, and A form when the nucleation temperature lower than T_D.

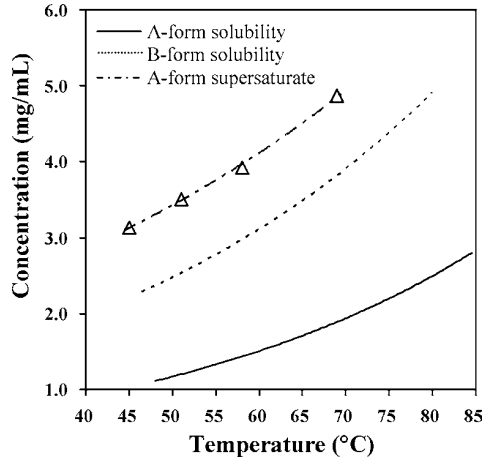

Figure 11. Experimental metastable zone width of polymorph A in acetonitrile.

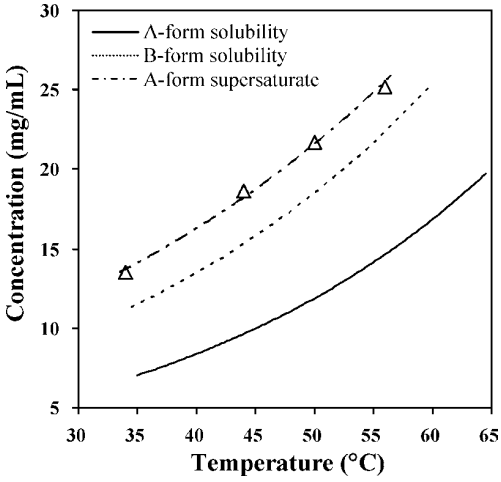

Figure 12. Experimental metastable zone width of polymorph A in methanol.

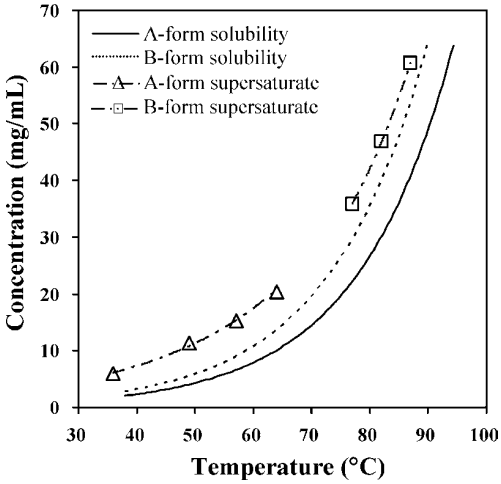

Figure 13. Comparison between experimental metastable zone widths of polymorphs A and B in water.

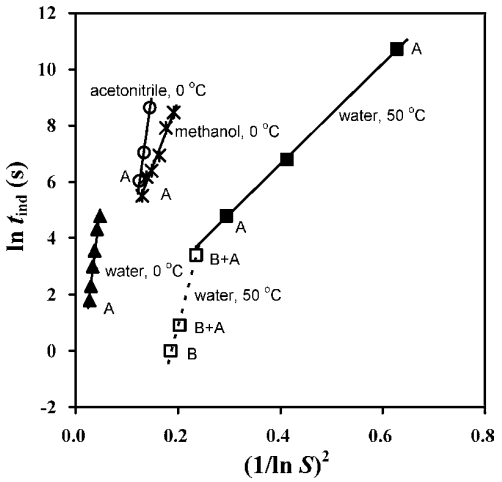

Figure 14. Dependence of induction time on supersaturation ratio, nucleation temperature, solvent, and the nature of the polymorph that crystallizes.

Table 2. Calculated Interfacial Tensions under Different Conditions

	interfacial tensions (mJ/m^2)			
T (°C)	water	acetonitrile	methanol	polymorph
0	15.68	14.88	10.70	A
10	13.08			A
20	12.37			A
50	9.16			A
50	14.36			B/B + A

Solvent-Mediated Transformation. In the suspension of pure B form, the transformation is not observed; this is because the solubility difference between form B and form A is not large enough to result in the nucleation of form A. In the presence of form A as seeds, form B can transform into the stable form A, though the kinetics is low, as shown in Figure 16. During the transformation process, the primary nucleation step is bypassed, and thus the transformation rate corresponds to the crystal growth rate of form A. For the growth of form A, the solution goes into an undersaturated zone with respect to form B, which makes it possible for form B to dissolve and produce a continuous supersaturation for form A to grow. The transformation will be complete when all of form B dissolves and the solution is saturated with respect to form A. On the other hand, as shown in Figure 16, the transformation rate remarkably increases with temperature. This trend confirms that this polymorphic system is monotropic and that form A is the thermodynamically stable form, whereas form B is the metastable form.[40]

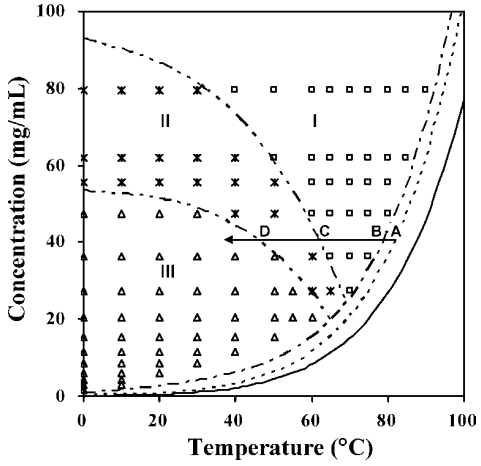

Figure 15. Effects of initial concentration and nucleation temperature on polymorphic crystallization behavior: Zone I, B form; Zone II, mixture of B and A forms; Zone III, A form; —, solubility curve of the A form; ···, solubility curve of the B form; —·—, supersaturate curve of the B form (high temperature) and A form (low temperature).

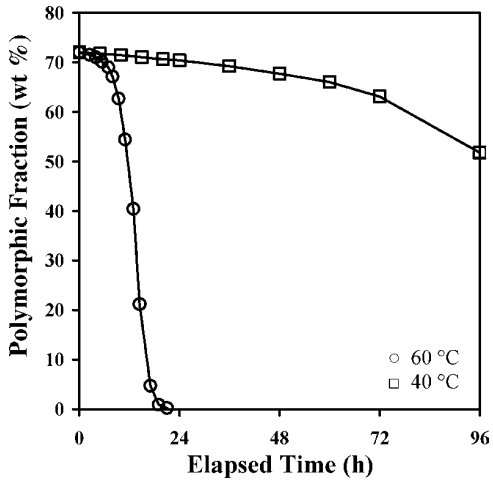

Figure 16. Polymorphic fractions of form B of famotidine in slurry as a function of time, at temperatures of 40 and 60 °C.

Table 3. Results from Cooling Crystallization Experiments without Seeding

	initial concentration (mg/mL)						
	water			methanol		acetonitrile	
cooling rate (°C/h)	60.8	40.7	6.6	28.8	18.5	5.0	3.1
2	B	B	A	A	A	A	A
12	B	B	A	A	A	A	A
20	B	B	A	A	A	A	A
60	B	B	A	B + A	A	A + B	A
ice bath[a]	B + A	A	A	B	A	B	A

[a] Quench-cooling by ice bath.

Cooling Crystallization without Seeding. Results from unseeded cooling crystallization experiments at different cooling rates and initial concentrations in water, methanol, and acetonitrile are presented in Table 3. It can be found that, when acetonitrile or methanol is used as solvent, the cooling rate can affect the polymorph of product only at high concentrations, that is, fast cooling crystallization from high concentration solution can produce polymorph B. However, when water is used as solvent, cooling rate has no effect on the polymorph of the final product.

Seeding Experiments. The polymorphs of products obtained from various seeding experiments are shown in Table 4.

As shown in Table 4, the efficiency of seeding can be influenced by the amount of seeds, cooling rate, and initial solution concentration. In general, slow cooling and an adequate amount of seeds can efficiently control the polymorph of the final product. And the higher the initial concentration and cooling rate, the more seeds required.

Discussion

From a thermodynamic viewpoint, for a polymorphic system, the minimization of ΔG is the classical thermodynamic driver, which leads to the formation of stable form, whereas the maximization of the rate of entropy production is the driver in irreversible thermodynamics, which will lead to the formation

Table 4. Results from the Seeded Cooling Crystallization Experiments in Water

cooling rate (°C/h)	initial concentration (mg/mL)	product form without seeding	seeds form	amount of seeds (wt %)	product form with seeding
20	6.62	A	B	5	B
2	6.62	A	B	5	B
20	6.62	A	B	2	B
2	21.98	A	B	5	B
2	21.98	A	B	2	B
20	21.98	A	B	2	B
20	21.98	A	B	5	B
20	61.75	B	A	5	A
2	61.75	B	A	5	A
2	61.75	B	A	2	A
20	61.75	B	A	2	B + A
2	61.75	B	A	1	B
20	75.77	B	A	1	B
20	75.77	B	A	5	B + A
20	75.77	B	A	30	A
2	75.77	B	A	5	A

of the less stable form. The equilibrium composition of the polymorphic mixture will depend on the rate at which excess energy is applied to the system.[41] From the viewpoint of structure, the polymorph which will crystallize preferentially from a melt or solution will be the one easiest to form (i.e., the one with the smallest energy barrier expressed in kinetic/thermodynamic terms) or the one whose structural organization is most readily derived from the arrangement in the melt or solution.[42] As shown in Figure 1 and Raman spectra, the polymorphism of famotidine can be mainly attributed to the conformational polymorphism. On the basis of the above viewpoints, the influence of crystallization parameters on the polymorphism of famotidine is discussed as follows.[43]

Initial Concentration. As to the effect of initial concentration, dependent on the total variation of nucleation and crystal growth rate, three types of behavior in a dimorphic system were recognized: (a) the more stable form would crystallize preferentially at all concentrations, (b) the less stable form would crystallize preferentially only at high concentrations, (c) the less stable form would crystallize preferentially only at intermediate concentrations.[44] As shown in Figure 15 and Table 3, the crystallization of famotidine belongs to type (b), that is, form B crystallizes preferentially only at high concentrations, whereas form A normally crystallizes from the solutions at low initial concentrations. In dilute solution, the interaction between solute molecules may be weak, so that conformer A extensively exists and preferentially nucleates. At high concentration, the interaction between solute molecules may be quite strong, and solute molecules exist in the conformation of conformer B.

Nucleation Temperature. At a certain concentration and a certain nucleation temperature, the supersaturation driving force is higher for polymorph A because it has the lower solubility, and the interfacial energy of the stable polymorph A is lower than that of the metastable polymorph B. From eq 2, assuming that the pre-exponential coefficient A_n and the geometric factor β are same, the polymorph A should thus be favored. However, when water was used as solvent (Figure 15), polymorph B crystallized preferentially at high nucleation temperature when the initial concentration was high enough. This is because, at high temperature, the collision frequency and interaction between solute molecules are largely increased, so that solute molecules favorably exist in the conformation of conformer B in solution or prenucleation aggregates.

Cooling Rate. Instinctively, it would be expected that slow crystallization from dilute solution would produce the stable form, whereas rapid crystallization from concentrated solution in which the kinetics could dominate would generate metastable forms. Our experiments show that, when acetonitrile or methanol is used as solvent, the cooling rate can affect the polymorph of the product only at high concentrations. That is because when a very fast cooling rate is employed, the metastable limit of polymorph B is exceeded, and thus polymorph B is preferentially formatted. In this case, the polymorphic purity of the product depends to a high degree on the nucleation rates of both forms. When the nucleation rate of form B is not high enough to consume the supersaturation quickly, form A can subsequently nucleate.

Solvents. Dependent on the conditions, crystallization of polymorphs from solvent may be under kinetic or thermodynamic control. In the latter case, the nature of the solvent will be immaterial in respect of the polymorph produced.[45] Nevertheless, specific solvent effects, which are related to the solvent−solute interactions and to bulk effects (e.g., interfacial tension) of the concentrated solution, are important in polymorph formation during crystallization.[46] The solvent−solute interactions can affect the nucleation, crystal growth, and solvent-mediated polymorph transformation,[47] which consequently affect the appearance of polymorphs. On the other hand, bulk properties of solvents, such as viscosity and surface tension, may also affect the crystallization kinetics and the appearance of polymorphs.[48] Besides, the solvent effect on crystallization has been interpreted in light of inhibiting nucleation or retarding crystal growth. In this respect, the phenomenon is analogous to controlling crystal morphology through additives and solvents.[49]

In many case studies in the literature, polar and nonpolar terminology has been used to address solvent effect on polymorphism.[50] However, hydrogen bonding may play a major role in that kind of effect. Hydrogen bonding can occur between solute−solute, solvent−solvent, and solvent−solute molecules. A solvent molecule that has a greater ability to donate or accept hydrogen bonding than the solute molecules will establish hydrogen bonding with the solute molecules and may not allow the other solute molecules to approach the same site. This will affect the final outcome of crystal structure and may even direct to a solvate formation.[51] Solvents with higher polarity index have more tendencies to disrupt hydrogen bonding between solute molecules.[52]

The solvent properties may be described by solvent property parameters, including hydrogen-bond acceptor propensity, hydrogen-bond donor propensity, polarity/dipolarity, dipole moment, dielectric constant, viscosity, surface tension, and cohesive

Table 5. Solvent Property Parameters of Water, Methanol, and Acetonitrile

solvent	π^a	$\Sigma\alpha^b$	$\Sigma\beta^c$	dipole moment (D)	dielectric constant	cohesive energy density (J mol mL^{-1})	viscosity[d] (mPa s)	surface tension[e] (cal mol^{-1} Å^{-2})
acetonitrile	0.75	0.07	0.32	3.92	35.69	522.95	0.37	41.25
methanol	0.60	0.43	0.47	1.70	32.61	808.26	0.54	31.77
water	1.09	1.17	0.47	1.87	78.36	2095.93	0.89	104.70

[a] Polarity/dipolarity of the solvent. [b] Summation of the hydrogen-bond donor propensities of the solvent. [c] Summation of the hydrogen-bond acceptor propensities of the solvent. [d] Viscosity of the solvent at 25 °C. [e] Surface tension of the solvent at 25 °C.

energy density, etc. Eight property parameters of three solvents used in this work are listed in Table 5.[53]

Our results show that solvents have effects on solubility, dissolution parameters, metastable zone width, and interfacial tension. Among three solvents studied, methanol provides the highest solubility and lowest interfacial energy, acetonitrile contributes lowest solubility and widest metastable zone width, and water results in the largest interfacial energy. On the other hand, from Table 5, water and methanol are known as dipolar protic solvents and can act as hydrogen-bond donors and acceptors. Acetonitrile is regarded as dipolar aprotic solvent and can act as hydrogen-bond acceptor. Water is more polar and the stronger hydrogen bond donor than methanol. As shown in Figure 1, the famotidine molecule has both hydrogen-bonding accepting and donating abilities. During cluster formation, the molecules can sit side-by-side and establish intra- and intermolecular hydrogen bonding between nitro oxygen atoms and the amine nitrogen atoms, such as intermolecular hydrogen bonds N4···N2, O1···N3, O1···N4 and intramolecular hydrogen bonds: N3···N1 and/or N3···N7.[54] The intramolecular hydrogen bonds play a decisive role in building the folded conformation, i.e., conformer B. Water, as the strongest hydrogen bond donor and acceptor, can provide the bridge bonded with the sulfamoyl N atom or O atom and with the guanidino N atom, which thus can further stabilize the folded conformation (conformer B), whereas methanol or acetonitrile cannot act as this kind of connector. Experimental results (Table 3) confirm that, when famotidine is crystallized from aqueous solution at high initial concentration, polymorph B (conformer B) can be produced, although methanol and acetonitrile with less hydrogen-bonding ability are preferred for crystallizing the stable polymorph A.

Seeds. Seeding can be used to control the product crystal modification. This control is effectively exercised during the nucleation phase by adding seeds of the desired form and thus overriding spontaneous nucleation.[55] On the basis of the results of this work, the efficiency of seeding is influenced by the amount of seeds, cooling rate, and initial solution concentration. The higher the initial concentration and cooling rate, the more seeds required. That is, the amount of seeds and the rate of crystallization should be balanced.

Conclusions

The polymorphism of famotidine possesses a monotropic nature and polymorph A is the thermodynamically favored form, whereas polymorph B is the kinetically favored form. The nature of the polymorph of famotidine that crystallizes from solution depends on the initial concentration of the solution, solvent, cooling rate, seeding, and nucleation temperature. Polymorph B crystallizes preferentially only at high concentrations. When acetonitrile or methanol is used as solvent, the cooling rate can affect the polymorph of product only at high concentrations. Although water is used as a solvent, the cooling rate has no effect on the polymorph, and the nucleation temperature is the predominant factor. The effect of crystallization conditions on the polymorph of famotidine is mainly attributed to its conformational polymorphism, which results from different types of intermolecular interactions of solute−solute and solute−solvent, e.g., hydrogen bonding. Besides, seeding can be used to effectively control the polymorph of final product. The efficiency of seeding is greatly influenced by the amount of seeds, cooling rate, and initial solution concentration. Last, in the presence of polymorph A as seeds, the transformation from polymorph B to polymorph A can proceed, and the rate increases with the temperature.

References

(1) Grant, D. J. W. In *Polymorphism in Pharmaceutical Solids*; Brittain, H. G., Ed.; Marcel Dekker: New York, 1999; pp 1−34.
(2) Henck, J. O.; Griesser, U. J.; Burger, A. *Pharm. Ind.* **1997**, *59*, 165−169.
(3) Ferrari, E. S.; Davey, R. J. *Cryst. Growth Des.* **2004**, *4*, 1061−1068.
(4) Ostwald, W. *Z. Phys. Chem.* **1897**, *22*, 289−330.
(5) Bernstein, J. *Polymorphism in Molecular Crystals*; Clarendon Press: Oxford, UK, 2002.
(6) Teychené, S.; Autret, J. M.; Biscans, B. *Cryst. Growth Des.* **2004**, *4*, 971−977.
(7) Ono, T.; ter Horst, J. H.; Jansens, P. J. *Cryst. Growth Des.* **2004**, *4*, 465−469.
(8) Jones, H. P.; Davey, R. J.; Cox, B. G. *J. Phys. Chem. B* **2005**, *109*, 5273−5278.
(9) Groen, H.; Roberts, K. J. *J. Phys. Chem. B* **2001**, *105*, 10723−10730.
(10) Beckmann, W. *Org. Process Res. Dev.* **2000**, *4*, 372−383.
(11) Donnet, M.; Bowen, P.; Jongen, N.; Lemaître, J.; Hofmann, H. *Langmuir* **2005**, *21*, 100−108.
(12) Laird, T. *Org. Process Res. Dev.* **2000**, *4*, 370−371.
(13) Weissbuch, I.; Addadi, L.; Lahav, M.; Leiserowitz, L. *Science* **1991**, *253*, 637−645.
(14) Davey, R. J.; Blagden, N.; Potts, G. D.; Docherty, R. *J. Am. Chem. Soc.* **1997**, *119*, 1767−1772.
(15) Agarwal, P.; Berglund, K. A. *Cryst. Growth Des.* **2003**, *3*, 941−946.
(16) Lu, J. J.; Ulrich, J. *Cryst. Res. Technol.* **2003**, *38*, 63−73.
(17) Lang, M. D.; Grzesiak, A. L.; Matzger, A. J. *J. Am. Chem. Soc.* **2002**, *124*, 14834−14835.
(18) Price, C. P.; Grzesiak, A. L.; Matzger, A. J. *J. Am. Chem. Soc.* **2005**, *127*, 5512−5517.
(19) Bonafede, S. J.; Ward, M. D. *J. Am. Chem. Soc.* **1995**, *117*, 7853−7861.
(20) Mitchell, C. A.; Yu, L.; Ward, M. D. *J. Am. Chem. Soc.* **2001**, *123*, 10830−10839.
(21) Hiremath, R.; Varney, S. W.; Swift, J. A. *Chem. Commun.* **2004**, 2676−2677.
(22) Zaccaro, J.; Matic, J.; Myerson, A. S.; Garetz, B. A. *Cryst. Growth Des.* **2001**, *1*, 5−8.
(23) Trask, A. V.; Motherwell, W. D. S.; Jones, W. *Chem. Commun.* **2004**, 890−891.
(24) Yu, L.; Ng, K. *J. Pharm. Sci.* **2002**, *91*, 2367−2375.
(25) Beach, S.; Latham, D.; Sidgwick, C.; Hanna, M.; York, P. *Org. Process Res. Dev.* **1999**, *3*, 370−376.
(26) Hilden, J. L.; Reyes, C. E.; Kelm, M. J.; Tan, J. S.; Stowell, J. G.; Morris, K. R. *Cryst. Growth Des.* **2003**, *3*, 921−926.
(27) Childs, S. L.; Chyall, L. J.; Dunlap, J. T.; Coates, D. A.; Stahly, B. C.; Stahly, G. P. *Cryst. Growth Des.* **2004**, *4*, 441−449.
(28) Ha, J. M.; Wolf, J. H.; Hillmyer, M. A.; Ward, M. D. *J. Am. Chem. Soc.* **2004**, *126*, 3382−3383.
(29) Gracin, S.; Rasmuson, Å. C. *Cryst. Growth Des.* **2004**, *4*, 1013−1023.
(30) Morissette, S. L.; Almarsson, O.; Peterson, M. L.; Remenar, J. F.; Read, M. J.; Lemmo, A. V.; Ellis, S.; Cima, M. J.; Gardner, C. R. *Adv. Drug Delivery Rev.* **2004**, *56*, 275−300.
(31) Hegedüs, B.; Bod, P.; Harsányi, K.; Péter, I.; Kálmán, A.; Párkányi, L. *J. Pharm. Biomed.* **1989**, *7*, 563−569.
(32) Overgaard, J.; Hibbs, D. E. *Acta Crystallogr., Sect. A* **2004**, *60*, 480−487.
(33) Ferenczy, G. G.; Párkányi, L.; Ángyán, J. G.; Kálmán, A.; Hegedüs, B. *J. Mol. Struct. (Theochem)* **2000**, *503*, 73−79.
(34) Stoica, C.; Tinnemans, P.; Meekes, H.; Vlieg, E. *Cryst. Growth Des.* **2005**, *5*, 975−981.
(35) Söhnel, O.; Mullin, J. W. *Colloid Interface Sci.* **1988**, *123*, 43−50.
(36) Datta, S.; Grant, D. J. W. *Cryst. Res. Technol.* **2005**, *40*, 233−242.
(37) Söhnel, O.; Garside, J. *Precipitation*; Butterworth-Heinemann: Oxford, UK, 1992.
(38) Tong, H. H. Y.; Shekunov, B. Y.; York, P.; Chow, A. H. L. *Pharm. Res.* **2002**, *19*, 640−648.
(39) Sato, K.; Boistelle, R. *J. Cryst. Growth* **1984**, *66*, 441−450.
(40) Giron, D. *Thermochim. Acta* **1995**, *248*, 1−59.
(41) Prigogine, I. *Thermodynamics of Irreversible Processes*; Wiley-Interscience: New York, 1955.
(42) Threlfall, T. *Org. Process Res. Dev.* **2003**, *7*, 1017−1027.
(43) Kitamura, M. *Cryst. Growth Des.* **2004**, *4*, 1153−1159.

(44) Cardew, P. T.; Davey, R. J. *Tailoring of Crystal Growth*; Institution of Chemical Engineers: Rugby, UK, 1982.
(45) Threlfall, T. *Org. Process Res. Dev.* **2000**, *4*, 384−390.
(46) Gu, C. H.; Young, V.; Grant, D. J. W. *J. Pharm. Sci.* **2001**, *90*, 1878−1890.
(47) Weissbuch, I.; Lahav, M.; Leiserowitz, L. *Cryst. Growth Des.* **2003**, *3*, 125−150.
(48) Mullin, J. W. *Crystallization*, 3rd ed.; Butterworth-Heinemann: London, 1993.
(49) Wireko, F. C.; Shimon, L. J. W.; Frolow, F.; Berkovitch-Yellin, Z.; Lahav, M.; Leiserowitz, L. *J. Phys. Chem.* **1987**, *91*, 472−481.
(50) Kamlet, M. J.; Dickinson, C. *J. Org. Chem.* **1982**, *47*, 4971−4975.
(51) Davey, R. J.; Allen, K.; Blagden, N.; Cross, W. I.; Lieberman, H. F.; Quayle, M. J.; Righini, S.; Seton, L.; Tiddy, G. J. T. *CrystEngComm* **2002**, *4*, 257−264.
(52) Mirmehrabi, M.; Rohani, S. *J. Pharm. Sci.* **2005**, *94*, 1560−1576.
(53) Gu, C. H.; Li, H.; Gandhi, R. B.; Raghavan, K. *Int. J. Pharm.* **2004**, *283*, 117−125.
(54) Golič, L.; Djinović, K.; Florjanič, M. *Acta Crystallogr., Sect. C* **1989**, *45*, 1381−1384.
(55) Beckmann, W.; Otto, W.; Budde, U. *Org. Process Res. Dev.* **2001**, *5*, 387−392.

CG060865+